

Experimental Behavior and Modeling of Wall-Diaphragm Connections for Older Masonry Buildings



T.J. Lin

National Center for Research on Earthquake Engineering, Taiwan

James M. LaFave

University of Illinois at Urbana-Champaign, USA

SUMMARY:

Wall-diaphragm connections can affect overall seismic performance of older unreinforced masonry buildings. Results are presented of an experimental study designed to evaluate the behavior of typical brick wall to wood joist / diaphragm connections. Tests were conducted on two different types of component specimens, using three different loading methods. Contributions of friction and of strap anchor nails loaded in shear have been considered separately and together in the testing matrix. Force vs. displacement hysteresis, envelope, and simplified average multi-linear curves have been developed from the experimental data. Moreover, representative curves can be obtained from these simplified average curves of the experiments to characterize more generally the overall behaviors (including compression contact between a joist and the masonry) typically exhibited by wall-diaphragm connections. A simple numerical model incorporating the structural phenomena of nails broken by shear force, compression forces, friction forces, and hysteretic behavior is also proposed.

Keywords: brick masonry; force vs. displacement curves; monotonic and cyclic loading; wall-diaphragm connection; numerical models

1. INTRODUCTION

Brick masonry can be an aesthetically pleasing, durable, and strong building material with good resistance to sound and thermal transmission. For these reasons, it has been a popular choice as a construction material for a variety of low-rise structural applications. However, unreinforced masonry (URM) structures can be relatively more vulnerable to earthquake excitations than steel, reinforced concrete, or even timber structures. During severe earthquakes, older URM buildings can exhibit a variety of damage mechanisms. In-plane and/or out-of-plane failures are the most likely damage modes for masonry walls. Local wall-diaphragm connection behavior may contribute to overall wall behavior, especially in the out-of-plane direction, depending on the nature of these connections. Early wall-diaphragm connections were often either star anchors or masonry anchors providing a positive attachment between the end of a wood floor joist and the brick masonry pocket in which it rested. One end of the steel anchor would be nailed to the web of a joist, with the other end embedded through the masonry wall to an external anchor plate. These types of anchors were typically only placed when a joist was perpendicular to and supported on a wall, but not for joists parallel to a wall. For global continuity of lateral load resistance in such structures, adequate overall connection is needed between the masonry walls and wooden floor diaphragms, which is typically provided by a mixture of the sort of connections described above along with other locations where the joists simply rest in brick masonry wall pockets.

A review of the literature has indicated that wall-diaphragm connections can have a significant influence on the seismic performance of URM buildings. Failure of the connections could lead to total structural collapse, and connection flexibility could significantly affect overall structural response. However, relatively little research has been conducted on the structural behavior of wall-diaphragm connections for URM buildings under various loadings, such as to even determine their basic force vs. displacement relationships. Due to this lack of data on inelastic force-displacement behavior of wall-diaphragm connections, an experimental study of representative wood joist and brick masonry

connections has been undertaken. The experimental data, such as overall force-displacement curves or even approximate stiffness values of connections, can then be used in developing numerical models of entire structures to better determine their response to ground motions.

2. TEST SET-UP

Nineteen wall-diaphragm connection test specimens were constructed by professional masons in the Newmark Structural Engineering Laboratory (NSEL) at the University of Illinois. Each specimen consisted of a small portion of brick masonry wall supporting a wood joist in a pocket joint, as shown in Fig. 1. Each subassembly consisted of eighteen clay bricks (with nominal dimensions of 10.16 cm × 6.78 cm × 20.32 cm) constructed using Type S Portland cement mortar, and the section of wood joist was nominally 5.08 cm × 30.48 cm (3.81 cm × 28.575 cm actual) and 60.96 cm. in length. Fifteen of the specimens had wall anchors made of a steel strap (30.48 cm × 3.81 cm × 0.3175 cm) and a threaded rod (1.27 cm dia. × 5 threads per cm. × 30.48 cm long), welded together. The wall anchor and wood joist were connected by two 10d (7.65 cm long) bright common nails, and the threaded rod was anchored outside the masonry with a standard hex nut and washer.



Figure 1. Test specimen of wall-diaphragm connection.

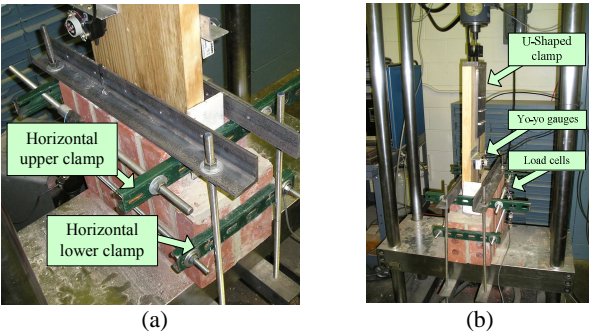


Figure 2. Clamping devices, displacement gages, and load cells.

The specimens were tested under uniaxial loading (in the joist longitudinal direction) in a testing machine. The brick masonry portion of the assembly was held down in place by two vertical clamps. Two additional horizontal steel clamps were used—a lower clamp to prevent the brick masonry assembly from cracking, and an upper clamp to apply a normal compression force between the joist and the base of the brick wall pocket, as shown in Fig. 2(a). Two load cells were used to measure the force in the upper clamp. This force was set to a representative value of around 3.78-4.0 kN at the beginning of each test, but was sometime varied during certain tests. The free end of the wood joist was attached to the actuator of the testing machine through a U-shaped clamp, as shown in Fig. 2(b). Two cable-extension position transducers (“yo-yo” gauges) were used to collect relative displacement data between the wood joist and brick assembly. Overall load (and displacement) data from the testing machine hydraulic actuator was also collected, as well as that from the two load cells.

3. TEST SPECIMENS AND TESTING METHODS

Two mechanisms of force transfer can exist in brick-joist wall-diaphragm connections. Mechanical connection is provided by nails that fasten the anchored steel strap to the wood joist, and frictional resistance exists between the wood joist and brick due to the loaded joists bearing on the wall. Therefore, some specimens were tested with only nails (6), a few with only friction (4), and even more with both mechanisms in play (9); a half-dozen specimens from this latter group were also tested further with only friction after the nails had failed, to supplement the other friction-only data. Tests were performed using three different methods – static (slow) monotonic loading, quasi-static cyclic loading (max. loading frequency = 0.02 Hz), and dynamic cyclic loading (loading frequency = 2 Hz).

4. TEST RESULTS

Based on the general descriptions provided above, the test specimens can be categorized by whether they had nails and friction (NF), nails only (N), or friction only (F), under different loading schemes. Since the key wall-diaphragm connections in real URM buildings resist loads by nailed straps that are connected to the wood and anchored through the masonry, test results for the NF case under static monotonic (SM) tension (opening) only, quasi-static cyclic (SC), and dynamic cyclic (DC) loadings will be emphasized, followed by some additional comparisons to N and F behavior. A listing of all specimens tested, including their type, loading, and failure mode / load, is given in Table 4.1. Force vs. displacement curves were obtained from conducting the experiments using the three different loading types. For ease of comparison, backbone envelope curves for cyclically loaded specimens were determined based on the peak points for each cycle. Then, average curves were obtained by further simplifying the envelope curves to piece-wise linear for the tension (joist pull-out) and compression (joist push-in) portion of behavior.

Table 4.1 Experimental Results of Test Specimens

Specimen Name	Failure Mode	Load Capacity (kN)	Displacement(s) when Two Nails Failed (cm)	Remark
NF_SM1	2 nails shear off at head	6.67	1.524, 3.302	*
NF_SM2	2 nails shear off at head	8.23	1.016, 1.524	*
NF_SC1	2 nails shear off at head	7.83	1.372, 1.448	*
NF_SC2	2 nails shear off at head	5.83	1.346, 1.905	
NF_SC3	2 nails shear off at head	8.41	0.914, 1.067	
NF_SC4	2 nails pull out	6.67	2.54 – 4.572	*
NF_SC5	1 nail shear off at head, 1 nail pull out	5.83	2.413 – 4.089	
NF_DC1	2 nails shear off at middle	7.56	0.305, 0.457	*
NF_DC2	2 nails shear off at head	8.45	1.016 – 1.143	*
N_SM1	2 nails pull out	6.74	3.556- 6.858	
N_SM2	1 nail shear off at head, 1 nail pull out	7.12	1.27, 4.064 – 6.096	
N_SC1	2 nails shear off at head	5.78	1.905, 2.337	
N_SC2	2 nails shear off at head	7.56	1.372, 1.930	
N_SC3	2 nails shear off at head	6.58	1.702, 2.235	
N_DC1	2 nails shear off at head	6.09	1.422 – 1.930	
F_SC1	-	-	-	
F_SC2	-	-	-	
F_DC1	-	-	-	
F_DC2	-	-	-	

Note: NF – nails and friction; N – nails only; F – friction only; SM – static monotonic; SC – static cyclic; DC – dynamic cyclic; * represents specimens tested further in friction after nails failed. (For some specimens, displacement at nail failure was not easy to distinguish, so a displacement range is given in such cases.)

4.1 Specimens including both nails and friction

At some wall-diaphragm connections in typical URM buildings, the floor joist has a metal strap nailed into it that is also connected through the masonry wall. Experiments on this category of specimen (NF), which included both nails and friction contributions, best reflect the behavior of this class of wall-diaphragm connection in URM buildings. The normal force (which was applied by the upper clamp) between the joist and the base of the brick wall pocket was equal to 4.0 kN in these cases. Structural response of this type of specimen when subjected to different loading situations is discussed in the sub-sections below.

4.1.1 Monotonic loading

Specimens NF_SM1 and NF_SM2 were each tested to failure under monotonic loading. They both failed as the two nails sequentially sheared off at the head. Failure of each nail was accompanied by a steep drop in the force vs. displacement curve, as may be seen in Fig. 3(a), with those key displacements and the overall maximum force given in Table 4.1. While specimen NF_SM2 had a larger load-carrying capacity, its nails were sheared off after going through smaller displacements (compared with specimen NF_SM1), which could be considered as less ductile behavior.

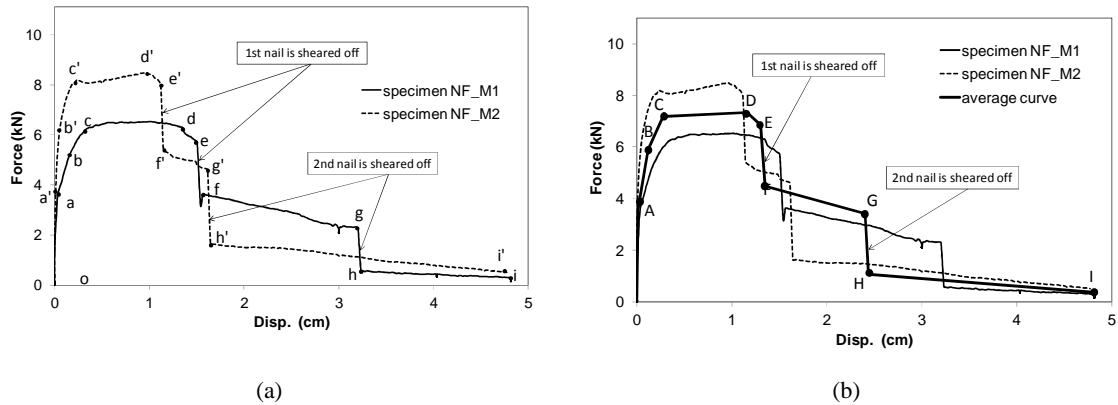


Figure 3. Force vs. displacement curves for type NF_SM specimens.

Prior to any significant “yielding”, these force-displacement curves could be approximated by three linear regions. When the connection is in a linear elastic state, lines $o-a$ and $o-a'$ can be chosen as the initial slopes for specimens NF_SM1 and NF_SM2, respectively. As the connection gets softer due to some modest local nail slip and prying into the wood joist, lines $a-b$ (and $a'-b'$) represent a second slope, followed by line $b-c$ (and $b'-c'$) chosen as the third slope. After the connection fully enters its yielding stage (related to shear yield and some additional prying of both nails), no obvious slope change is seen across a fairly wide range of displacements, with point d chosen as the end of this “yield plateau”. After that, the connection begins to soften even further, exhibiting negative stiffness as the first nail approaches a combined shear / tension failure culminating in its fracture ($d-e-f$). The connection then again becomes somewhat more stable for a time until the second nail also fails ($f-g-h$), after which all that remains is some very modest resistance (approximately 0.89-1.33 kN) attributable only to friction ($h-i$). By taking an average of the force and displacement values for each of points a through i (and their a' through i' counterparts), points A through I can be obtained, as shown in Fig. 3(b) connected as a multi-linear average representing these two monotonic tests having nails and friction.

4.1.2 Quasi-static cyclic loading

Five specimens were tested with nails and friction under quasi-static cyclic loading. The ultimate failure mode for specimens NF_SC1, NF_SC2, and NF_SC3 was two nails shearing off at the head, after some modest slip, prying, and yielding (similar to as earlier for specimens NF_SM1 and NF_SM2). For specimen NF_SC4, the eventual failure mode was both nails fully pulling out, and in specimen NF_SC5 one nail sheared off at the head while the second one pulled out. Behavior of all these type NF wall-diaphragm connections under quasi-static cyclic loading is next discussed, in part as a function of the failure modes of nails shearing off vs. nails pulling out.

4.1.2.1 Failure mode of nails shearing off

Three specimens (NF_SC1 through NF_SC3) failed as both nails sheared off. A sample cyclic force vs. displacement curve (for specimen NF_SC2), shown in Fig. 4(a), is qualitatively fairly representative of this type of behavior. Maximum resistance of around 5.78 kN was achieved at a

displacement of about 0.635 cm, with two later drops in load at about 5.12 kN and 2.89 kN (at displacements of around 1.27 cm and 1.905 cm) representing the two nails shearing off at the head. After the nails sheared off, only the friction force is left, which was around 1.11 kN in the later cycles. The unsymmetrical behavior of the hysteresis curve in compression vs. tension is due to the wood joist end eventually coming to bear (sometimes at modest displacements, generating fairly large forces) on excess mortar droppings in the gap between the wood joist and the bricks when the wood joist moves toward the brick assembly. In order to simplify the type of hysteretic force vs. displacement curve shown in Fig. 4(a), the maximum points can be picked out for each cycle and all connected to form an envelope curve. The so-called “average” curve, shown only in the joist pull-out (tension) direction of loading, is then simply made as a piece-wise linear version of the envelope.

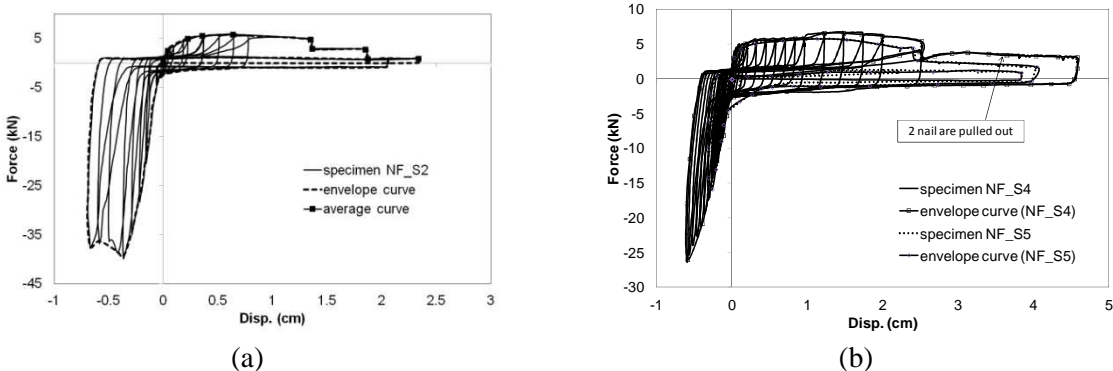


Figure 4. Force vs. displacement, envelope, and average curves for: (a) specimen NF_SC2, (b) NF_SC4 and NF_SC5.

4.1.2.2 Failure mode of nails pulling out

Specimens NF_SC4 and NF_SC5 each had part of their failure mode controlled by nail(s) pulling out of the wood joist, rather than only by nail shear failure (in NF_SC4, both nails pulled out, while in NF_SC5 one nail sheared off and another one pulled out). This failure mode (see Fig. 4(b) for the load-displacement data) appears to be a bit more ductile than in other NF_SC specimens that had their behavior governed by both nails shearing off. In these two specimens, which exhibited quite similar behavior to one another (in spite of their slightly different failure modes), there was a noticeable drop in load-carrying capacity at a displacement of around 2.54 cm in NF_SC4 this was due to partial pullout of both nails, whereas in NF_SC5 it was a reflection of one of the nails fracturing. Subsequent behavior in each case (up to failure at displacements of about 3.6-4.445 cm) is then entirely related to nail pullout, after which only a frictional capacity of about 0.89- 1.11 kN remained.

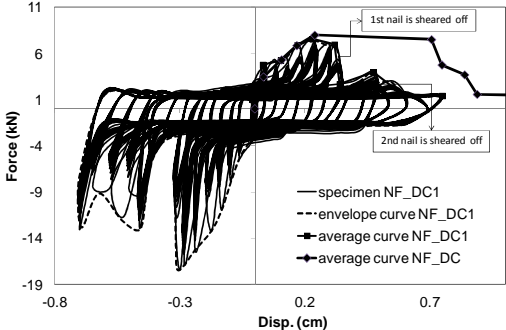


Figure 5. Dynamic cyclic force vs. displacement (and envelope) curves.

4.1.3 Dynamic (cyclic) loading

Dynamic behavior of the NF test specimens was a little bit different from their static behavior.

Dynamic loading was typically in groups of ten cycles at constant amplitude, starting from a target of about ± 0.0508 cm and then increasing in whole number multiples of that from there. Specimens NF_DC1 and NF_DC2 each exhibited an ultimate failure mode of both nails shearing off, albeit at lower ultimate displacements than otherwise similar failures of type NF_SM and NF_SC specimens. An example (for NF_DC1) of dynamic load-displacement behavior is shown in Fig. 5, where it may also be seen that the dynamic structural response is similar to the behavior in the static cyclic case (especially when nails sheared off).

4.1.4 Representative curves of NF category

For all type NF specimens (regardless of failure mode), envelope load-displacement curves under static monotonic, static cyclic, and dynamic cyclic loading (representing all failure modes) are compared in Fig. 6. Connection behavior of the NF_SM and NF_SC tests are quite similar, especially in terms of overall capacity and the force when each nail failed. NF_SM tests exhibited the greatest ductility, while NF_DC tests had the least (but were also the strongest, on average). By taking an average of the force and displacement values for each key point composed of envelope curves of NF_SM, NF_SC, and NF_DC, points A through I can be obtained, as shown in Fig. 6 connected as a multi-linear “average” curve of NF category in tension. In order to simplify the average curve of NF category, so called “representative” curve is made by picking up the points at the average curve based on obvious stiffness changing. Curve *oa* is the initial slope with the same slope with curve *OA*. Then, curve is extended by following the slope of curve *AB* until reaching the load value as same as point *D*, as curve *ab*. After that, maintain the horizontal curve *bc* with the maximum loading capacity of wall-diaphragm connections around 7.43 kN. The first drop, as curve *cd* following the slope of curve *EF* represents the first nail failed. The connections were continually pulled away from the wall, shown as horizontal curve *de* until the second nail failed which represented by curve *ef*. Both nails have the same resistance which is equal to 3.11 kN. After two nails failed, only friction force (1.2 kN) is left as shown as horizontal curve *fg*, which can be decided by taking an average of displacement and force values for points *H* and *I*.

The compressively representative curves of NF_DC and NF_SC, shown in Fig. 7 can be obtained by the same rules which are applied to the tensile behavior. It can be found connections of NF_DC were only moved with mortar dropping without crushing the wall. By taking an average of the values between points 1 and 1', and points 2 and 2', curve *cd* can be decided. Once displacement is over the value of point *d*, the representative curve follows the curve of NF_SC at the stage of hitting the wall. Curve *ab* represents the initial compressive force provided by nails (around 3.74 kN) before the connection gets softer due to some modest local nail slip. By connecting with points *a* through *f*, the representative curve of NF category in compression can be obtained.

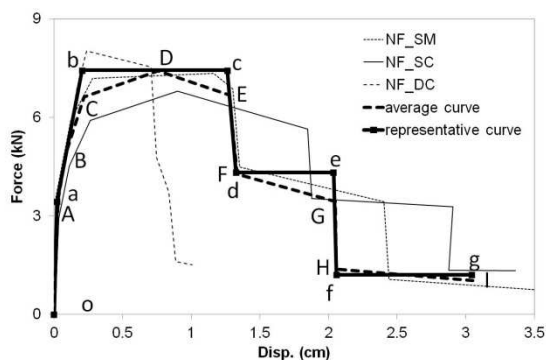


Figure 6. Representative curves of NF category in tension.

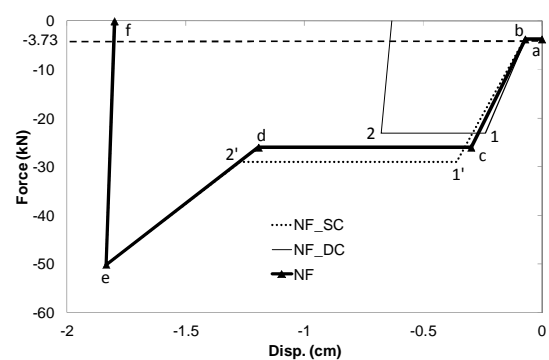


Figure 7. Representative curves of NF category in compression.

4.2 Specimens including nails only

For this type of connection (N), only nails connected the wall (through the strap anchor) to the wood joist (without any clamping normal force acting on the connection to enable a frictional contribution). This connection scenario may not reflect any particular real one in a URM building, but it can be used to better understand experimentally the behavioral contributions of just the nails to overall connection performance. Fig. 8 shows overall average curves for the N_SM, N_SC, and N_DC tests, where there are recognizable trends both among these behaviors and also compared with those of the respectively similar type NF tests. The load-carrying capacity of type N specimens was typically up to 10-20% less than in companion NF tests, while their displacements at nail failure were generally a bit greater.

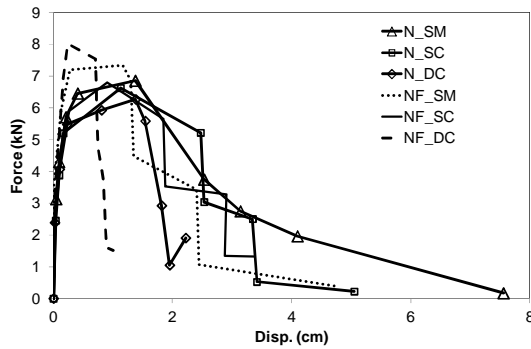


Figure 8. Average envelope curves for specimens with nails only vs. with nails and friction.

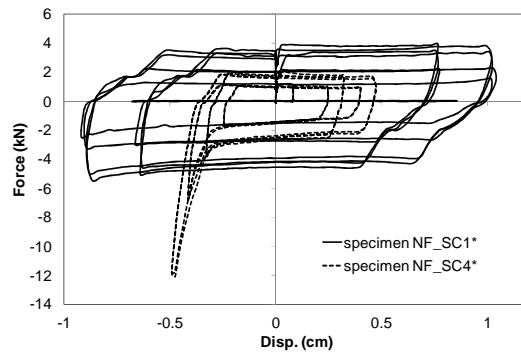


Figure 9. Force vs. displacement curves for specimens NF_SC1* and NF_SC4*.

4.3 Specimens including friction only

Only friction was acting on specimens under static and dynamic cyclic loading for this kind (F) of connection, which represents a common case in URM buildings of many joist-pocket connections without strap anchors. As can be seen in Fig. 9, force vs. displacement curves obtained for specimen NF_SC1* are more symmetric than in NF_SC4* (which had higher compression forces). This latter behavior is attributed to the wood joist eventually coming into contact with excess mortar dropped into the gap between the wood joist end and the bricks, generating large forces when the wood joist moves far enough toward the brick assembly.

5. MODELING OF WALL-DIAPHRAGM CONNECTIONS UNDER CYCLIC LOADING

As the above discussion, the overall representative curves of wall-diaphragm connections can be obtained by representative (envelope) curves which describe the tensile and compressive behaviors of different type connections. In this section, the rules which can simplify hysteretic curves and decide cyclic loading paths were proposed based on experimental data of testing specimens. These rules can be applied in the numerical simulation described latter as well.

5.1 Tension

The hysteretic behavior of connections under cyclic loadings in tensile part can be described by the following rules. The representative curve *o-g* shown in Fig. 10(a) is regarded as an overall envelope curve of NF category. Connections which are in the elastic stage are unloaded along curve *oab* as loaded. Once connections enter into the plastic stage, cyclic paths are assumed starting from point 1, where only friction force acted (with nails). After that, path is going along curve *1, 6* (elastic), curve *6, 7* (hardening) then unloading along curve *7, 3, 11* until negative friction force left. The nails have gradually loosened by previous cyclic loadings. Thus, next cycle would start from point 2, which was decided at previous second cycle. Connections enter into the elastic stage along curve *2, 7*, in which point 7 has already determined by last circle. After that, connections go into hardening and then

are unloaded along points 7, 8, 4, and 12. The following circles follow the same rules until cyclic paths are over point 9, which can be decided from observations of experimental data. After that, the following cyclic paths start from point 4 and the stiffness of connection is decreasingly softer with increasing cyclic circles.

5.2 Compression

The cyclic compressive behavior of connections is followed the same rules proposed in section 5.1 (tension) as well. The representative curve $a-f$ of NF, shown in Fig. 10(b) is regarded as the envelope curve of cyclic loading paths. The cyclic paths of connections are assumed to start from point a (with negative friction force only), and then enter into elastic and hardening stages along curve ab and $b8$. After that, connections are unloaded along points 8, 2, and 13 until only positive friction force left. So are the cycles along with points 2, 8, 9, 3, and 14 and points 3, 10, 11, 5, and 16. Once a wood joist crushed the wall, it produces highly compressive forces as the cycle follows along points 6, 12, 13, 7, and 17.

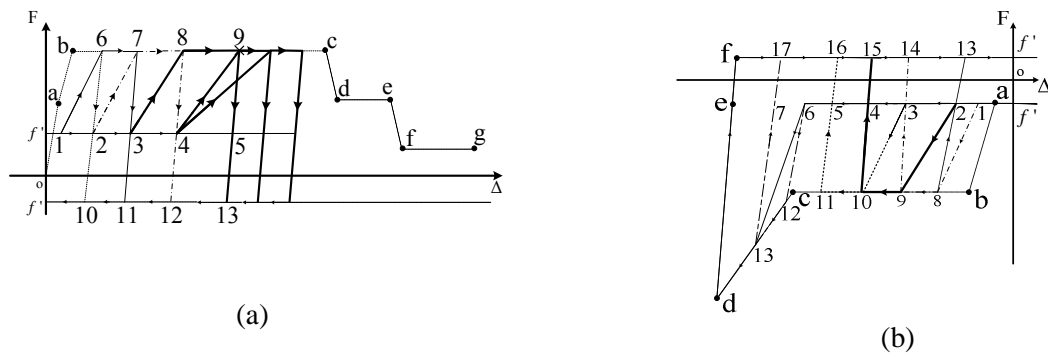


Figure 10. Cyclic loading paths at force vs. displacement curves: (a) Tension; (b) Compression.

6. NUMERICAL ANALYSIS

A simple numerical model of wall-diaphragm connections is necessary for use in the FEM simulation of an overall building. A model including nails, friction, and contact, shown as Fig. 11 is proposed for the simulation of structural behavior of connections under monotonic and cyclic loadings.

Two nails are simulated by two parallel springs, which was assumed two springs have the same loading capacities ($f_1 = f_2$ in tension), shown as Fig. 12. To reflect the failure mode of two nails shearing off in order, the ductility of the second nail is larger than the first one, which means the second nail resists external force after the first nail was sheared off. The strength of springs can be adjusted according to the value of friction forces. From the representative curve of NF category obtained from section 4.1.4, the strength of nails is equal to 3.11 kN when friction force is 1.20 kN. Friction force proposed in Fig. 13 describes two different situations of friction forces exist in the connections. It is assumed positive friction forces are same as negative ones. In Fig. 13(a), the value of F_1 which denotes friction forces before two nails are broken (with nails) is larger than the one of F_2 which denotes friction forces after two nails are broken (without nails). $F_{rep.}$ (2.02 kN) obtained by taking an average between F_1 and F_2 , is recommended as friction force in numerical simulation of NF category under cyclic loadings, shown in Fig. 13(b). Contact model was proposed to describe the behavior of a wood joist in compressive behavior. As shown in Fig. 14, the envelope curves of models A-B represent three different stages of wall joists. The behavior of a wood joist from moving into gap, then crushing the mortar, and finally moving far enough to hit a wall pocket can be simulated by models A, B, and C, respectively. f_3 , f'_3 , f''_3 , Δ_3 , Δ'_3 , and Δ_3'' represent the maximum compressive

force and negative displacement at A, B, and C models.

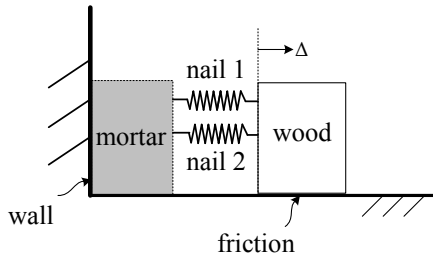


Figure 11. The details of numerical model

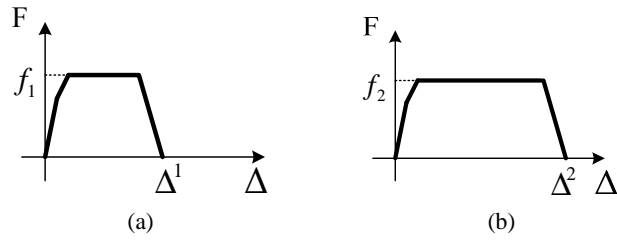


Figure 12. Force and displacement curves (a) first spring; (b) second spring.

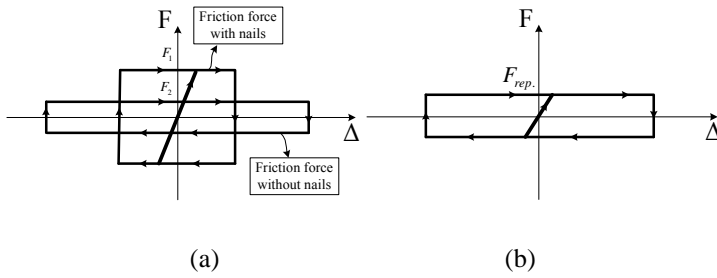


Figure 13. Friction model: (a) friction model; (b) average friction model.

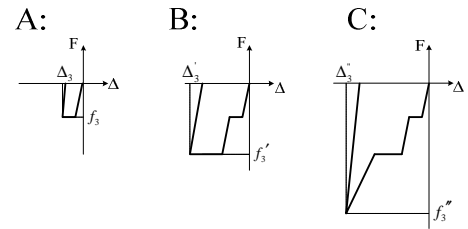


Figure 14. Contact model.

7. NUMERICAL RESULTS

Based on the numerical model proposed above, the rules of cyclic paths proposed in section 5 are applied to the establishment of the force and displacement hysteretic curves. As can be seen, the stiffness of connection in tension direction is getting softer with increasing cyclic circles when displacement of cyclic path is over 0.2". For simplification, friction force equal to the absolute value of 2.03 kN in tension and compression directions is adopted either two nails are broken or not. The strength of each spring is assumed as 2.7 kN which can be obtained from the information of the loading capacity of connections (7.43 kN) and friction forces (2.03 kN). Compared with the experimental data of NF_SC1, and NF_DC1 shown in Figs. 15(a) and (b), the numerical results with representative friction models can catch up most of structural behavior of connections in tension, such as maximum loading capacity, friction forces, and cyclic paths. In addition, the representative cyclic behavior in compression shown by the numerical model can include the realistic behavior of connections of NF_SC1 and NF_DC1 when the joists crush with dropping mortar.

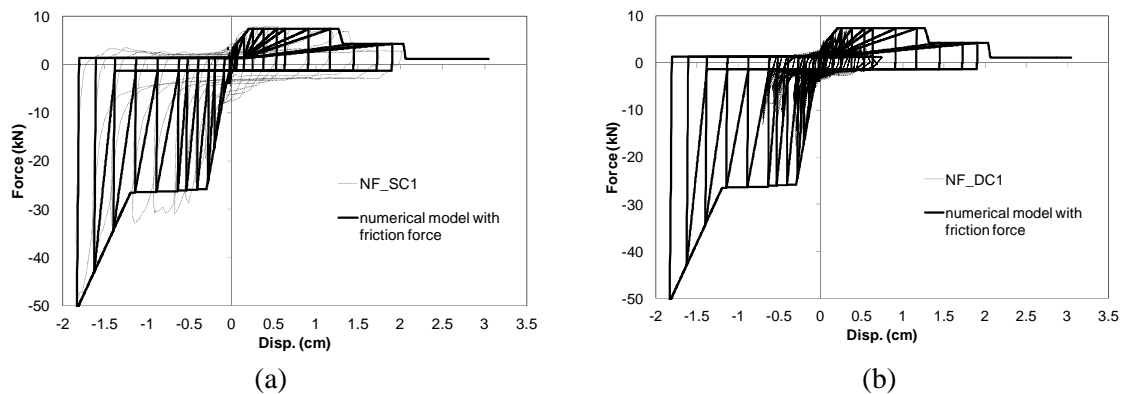


Figure 15. Force vs. displacement curves: (a) NF_SC1; (b) NF_DC1.

8. CONCLUSION

Seismic performance of brick masonry buildings can be affected by vulnerable wall-diaphragm connections. For older URM buildings, nails that fix a steel strap to certain wood joists are an important element of wall-diaphragm connection structural behavior, as is friction. By conducting experiments on representative wall-diaphragm connections under different loading schemes, their force vs. displacement behavior (including average envelope curves) has been developed. For the case of connections with both nails and friction, which represent many typical URM building joist-brick connections, behavior of the wall-diaphragm connection under dynamic cyclic loading was more brittle than behavior under monotonic or quasi-static cyclic loading. Average load-displacement curves of those latter NF connections under monotonic and quasi-static loading were fairly coincident with one another and also with those of most specimens resisting force by virtue of nails only. Test results of all specimens with nails indicate that their strength typically ranged from about 5.78 to 8.45 kN. The hysteretic behavior of specimens is investigated in this work as well. Based on observations of experimental data, overall cyclic loading paths can be concluded to some rules. By following these rules, the representative cyclic curves obtained from the numerical models which consist of two nails, friction, and contact are proposed to catch the behavior of connections under different loading types. Two nails are simulated by two springs which have the same loading capacity with different ductility. Contact modes based on the compressive representative curves can describe the overall compressive behavior of connections at different stages. Two friction models proposed here can be applied into the NF category with/without nails. An average value of friction force was proposed by simply taking an average of friction forces provided by two models. The numerical results can well represent the overall tensile and compressive behavior of a wall-diaphragm connection. Moreover, the numerical model could be used to simulate nonlinear finite element models of whole buildings in the future.

ACKNOWLEDGEMENT

This work was funded in part through the Mid-America Earthquake (MAE) Center, under a grant from the Earthquake Engineering Research Centers Program of the National Science Foundation per Award No. EEC-9701785. The authors would like to thank NSEL research engineer Greg Banas and University of Illinois graduate student Zhongzhuo Li for their assistance with the laboratory testing.

REFERENCES

- Costley, A.C., and Abrams, D. (1995). Dynamic response of URM buildings with flexible diaphragms. Thesis Report. Civil Engineering, University of Illinois at Urbana Champaign.
- Cross, W.B., and Jones, N.P. (1993). Seismic performance of joist-pocket connections. Part I : Modeling. *Journal of Structural Engineering*. **119:10**, 2986-3007.
- Cross, W.B., and Jones, N.P. (1993). Seismic performance of joist-pocket connections. Part II : Application. *Journal of Structural Engineering*. **119:10**, 3008-3023.
- Karapitta, L., Mouzakis, H., and Carydis, P. (2011). Explicit finite-element analysis for the in-plane cyclic behavior of unreinforced masonry structures. *Earthquake Engineering and Structural Dynamics*. **40:2**, 175-193.
- Li, M., Foschi, R. and Lam, F. (2012). Modeling Hysteretic Behavior of Wood Shear Walls with a Protocol-Independent Nail Connection Algorithm. *Journal of Structural Engineering*. **138:1**, 99-108.
- Lin, T.J. and LaFave, J.M. (2011). Experimental Structure Behavior of Wall-Diaphragm Connections for Older Masonry Buildings. *Construction and Building Materials*. **26:1**, 180-189.
- Peralta, D.F., Bracci, J.M., and Hueste, M.D. (2004). Seismic Behavior of Wood Diaphragms in Pre-1950s Unreinforced Masonry Buildings. *Journal of Structural Engineering*. **130:12**, 2040-2050.
- Simsir, C.C., Aschheim, M.A., and Abrams, D.P. (2004). Out-of-plane dynamic response of unreinforced masonry bearing walls attached to flexible diaphragms. 13th World Conference on Earthquake Engineering, Vancouver, B.C., Canada.
- Yi, T., Moon, F.L., Leon, R.T., and Kahn, L.F. (2006). Analyses of a Two-Story Unreinforced Masonry Building. *Journal of Structural Engineering*. **132:5**, 653-662.